IJAME

Int. J. of Applied Mechanics and Engineering, 2024, vol.29, No.2, pp.1-15
DOI: 10.59441/ijame/186684

MODEL ANALYSIS OF WORM GEAR PAIR SYSTEM USING FINITE ELEMENT ANALYSIS

Raghavendra Rajendra Barshikar*
Department of Mechanical Engineering, MET BKC Institute of Engineering, Nashik, INDIA
E-mail: raghavendrabarshikar@gmail.com

Prasad R. Baviskar and Milind M. Patil
Department of Mechanical Engineering,
Sandip Institute of Technology and Research Center, Nashik, INDIA

Anil S. Dube
Department of Mechanical Engineering, Sandip Institute of Engineering and Management, Nashik, INDIA

Vishal J. Dhore
Department of Mechanical Engineering,
Guru Gobind Singh College of Engineering and Research Center, Nashik, INDIA

Spur gear, helical gear, worm gear, and bevel gear are all important components in industrial applications such as vehicles, pushes, conveyors, elevators, bowl mill, rolling mills, ribbon blender, machine tools, aeroplanes, and windmills. When various types of defects, such as wear, tooth breakage, corrosion, and scratches on bearings, appear in gearboxes, normal machine function may be abruptly terminated. As a result, output and dependability suffer. As a result, several quality tracking and evaluation approaches have been adopted by companies. Finite element analysis (FEA) is one of the approaches. This research paper presents the FEA of a ribbon blender worm gear pair by using Ansys 18.0 to identify the weak gear of the worm gear pair, natural frequency, and deformation. Proe-5 utilized for creation of three-dimensional geometry of threaded worm and toothed worm wheels, as well as other related elements such as shafts and bearings. Steel is used for the worm, shaft, and bearing, whereas bronze is used for the worm wheel. Ansys 18.0 is implemented to carry out worm gear pair model analysis. The results demonstrate that the worm wheel had the most deformation when compared to the worm, and that the natural frequency is greater than the operational frequency of the worm gear pair. The findings of the research study, worm wheel deteriorate early than worm, model analysis plays a significant role in vibration monitoring of worm gear pair, and this work is valuable for further fault analysis of ribbon blender worm gearbox utilizing vibration response.

Key words: worm gear pair, finite element analysis, model analysis, deformation, natural frequency.

1. Introduction

The dynamic load is a major worry for speed transmitting elements such as pinion gear pair, worm gearbox, helical gear, shaft, bearings, pulleys, keys, and so on. In gears, dynamic load causes bending stresses at the tooth root, which can lead to premature failure. A reduction of dynamic load is an essential issue in the design of speed transmission gears [1]. Model analysis plays a crucial role in analysing dynamic load imposed on gears. The most fundamental type of dynamic evaluation, known as a modal analysis, identifies the natural frequencies at which a structure would vibrate [2]. Most of literatures utilized finite element analysis (FEA) for model analysis. FEA is a numerical approach for analysing the dynamics of mechanical systems, such as pinion gear pair, worm gearbox, helical gear, shaft, bearings. When a high gear ratio and speed reduction

* To whom correspondence should be addressed

between two perpendicular shafts is required, a worm gear box, which is made up of a worm screw and worm wheel (also known as a worm gear wheel), plays a crucial role in speed transmission [3]. Worm gearbox benefits include their compact size, easier construction, self-locking action, and less backlash. This worm gearbox is made with high precision. Worm gearbox is used for increasing torque or to reduce the speed. It is almost impossible to reverse direction of power by using worm gearbox because of the high friction between the worm and worm wheel. In general, the harder the worm the greater the strength and wear resistance. Material for the worm therefore calls for a hard surface and core strength. Thus worms are made of case hardened steel. The varieties of steel are used for the worm are *40C8*, *55C8*, *10C4*, *14C6*, *16Ni80Cr60*, *20Ni2Mo25* [4].

In worm gearbox, as the material of worm screw is generally harder than that of worm wheel, worm wheel gear can wear out, get pitted, or even experience tooth breakage during sliding. This raises concerns about the worm gearbox's worm wheel gear failure [5-6]. FEA is frequently used for model analysis of worm gearboxes. There are several faults that can arise on a worm wheel, including scoring, abrasive wear, and tooth breaking [7-8]. Londhe *et al.* [9] by using finite element analysis, examined the bending stress in the worm gearbox of a winch machine. The outcome demonstrates that while the worm wheel's design is secure, production errors lead it to break down while in operation. Additionally, worm produced using a milling machine performs better than one made on a lathe. Honkalas *et al.* [10] concentrated on the soot blower, its application, and its functionality. The worm and worm wheel of the gear motor used in the soot blower determine how well it works. The existing design of the worm and worm wheel was effectively examined using the finite element analysis approach. To avoid a vibration condition, Jibhakate *et al.* [11] estimated the natural frequency of the synchromesh gear mesh system using the Holzer technique and the finite element method (FEM). The outcome demonstrates effectively and successfully the FEM approach determines natural frequency. Through experimental and finite element analysis (FEA), Bhat *et al.* [12] examine the worm gear pair's different features, such as lubrication, wear, and friction. Research result shows that there is a *16÷22* % difference between experimental and FEA results. Mohamed *et al.* [13] to ascertain the variation in stiffness with regard to the angular location for various combinations of crack lengths, a finite element analysis was carried out. Maheedhara and Pourboghrat [14] examined worm gearboxes utilised in car power windows and windscreen wipers. Finite element analysis is used to calculate the size of the composite worm under static loads and constant temperature. Dynamic load and bending stress at helical gear tooth are calculated using finite element analysis (FEA), photo stress coating, velocity factor technique, and Spott's equation method. The outcome demonstrates that, in comparison to other methods, FEA reliably examines the worm wheel [15]. In the examination of the worm gear pair model, finite element analysis is crucial [16]. According to Tao *et al.* [17] at the beginning stage of gear meshing, excessively high impact in the worm drive generated an initial breakage at the root location of softer worm gear. Model investigation of a ribbon blender's worm gear pair is done in the current study. The worm gear pair's various dimensions were established through a methodical design process. Ansys 18.0 is used to determine the natural frequency and deformation of six models, including the worm and worm wheel, worm and worm wheel, worm wheel twisting, worm wheel complex bending, and worm wheel twisting modes. The worm and worm wheel is modelled according to the dimensions in Proe-5. Calculated operating frequency based on *2880 rpm* input speed.

The current research article is divided into three sections: methodology, discussion of the findings, and conclusion. The technique section shows a FEA of a worm gear pair to calculate the natural frequency, deformation, and operating frequency. The findings of the study are detailed in the results and discussion section. The conclusion section summarises the outcome.

2. Methodology and material

2.1. Methodology

The following steps comprise the methodology used in this study.

1. Calculation of Dimensions of ribbon blender worm gearbox and operating frequency based on *2880 rpm* input speed.

2. Creation of three dimensional model of worm and worm wheel according to the dimensions in Proe-5 software.
3. Development of a FEA model of a worm and a worm wheel, including mesh creation, material property assignment, and boundary condition application.
4. Determination of natural frequency and deformation through FEA.
5. Discussion of the findings, and conclusion.

2.2. Finite element analysis (FEA)

Finite element analysis (FEA) is a use of computations, models, and simulations to estimate and analysed how an item can react under various physical situations. Different type of analysis carried out by using FEA such as Structural analysis, thermal analysis, model analysis and seismic analysis [12]. Different software are available to performed FEA like Abacus, Nastran, Radios, and ANSYS Workbench. Most of researcher utilised ANSYS Workbench as compared to other software's.

2.3. Ribbon blender worm gearbox

Ribbon blender are a form of powder blender that is made up of two components that are positioned on a central shaft. Worm gearbox is the vital component of ribbon blender as they required different speed. They are most typically employed for solids-on-solids mixing, but they may also be used for coating a dry particle with a liquid component or particle absorption of a liquid addition.

Fig. 1. Ribbon blender worm gearbox

(a)

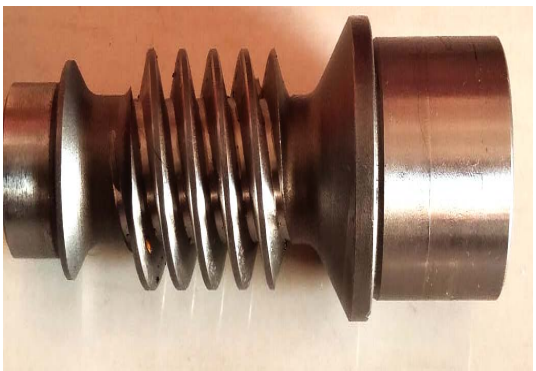

(b)

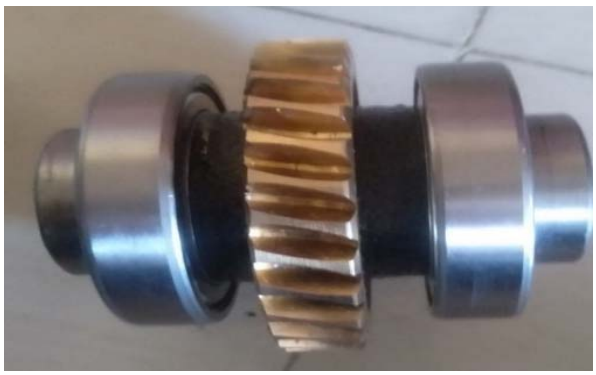

Fig.2. Internal parts of worm gearbox: (a) worm, (b) worm wheel.

In this research work ribbon blender single stage worm gearbox as shown in Fig.1 is considered for model analysis. Worm and worm wheel are as depicts in Fig.2. As the worm gearbox runs at a *2880 rpm*, the operational frequency is *48 Hz*.

2.4. Calculation of dimensions of worm gearbox

Company specification:

Z_w : number of starts of the worm $= 2$,

Z_g : number of teeth of the worm wheel $= 30$,

φ : helix angle $= 12°31'43''$,

m_n : normal module $= 2.5$.

Worm bearing number $=$ *6204-2RS*, *6006*.

Worm wheel bearing number $=$ *6008RS*.

Helix angle φ :

$$1° = 60',$$

$$31' = \frac{31}{60} = 0.5166°, \tag{2.1}$$

$$43'' = \frac{43}{3600} = 0.0119°, \tag{2.2}$$

$$\varphi = 12° + 0.5166° + 0.0119 = 12.52°, \tag{2.3}$$

$$\varphi = 12.52 \times \frac{\pi}{180}, \tag{2.4}$$

$$\varphi = 0.2185^{c}.$$

Module *m*:

$$m_n = m\cos\varphi, \tag{2.5}$$

$$2.5 = m\cos(12.52),$$

$$m = \frac{2.5}{\cos(12.52)},$$

$$m = 2.5 .$$

Gear ratio $= 15$.

Worm gears pairs specified as:

$$Z_w / Z_g \ / q / m$$

where *q*: diametral quotient $= 10$ [18].

Axial pitch P_x :

$$P_x = \pi \times m , \tag{2.6}$$

$$P_x = \ \pi \times 2.5 ,$$

$$P_x = 7.85 ,$$

$$P_x \approx 8 \ mm .$$

Lead l :

$$l = \ P_x \times Z_w , \tag{2.7}$$

$$l = 8 \times 2 ,$$

$$l = 16 mm .$$

Pitch circle diameter of the worm $\left(d_w\right)$:

$$d_w = q \times m , \tag{2.8}$$

$$d_w = 10 \times 2.5 = 25 mm ,$$

Pitch circle diameter of worm wheel $\left(d_g\right)$:

$$d_g = m \times Z_g , \tag{2.9}$$

$$d_g = 2.5 \times 30 .$$

Centre distance *a*:

$$a = \frac{d_w + d_g}{2}, \tag{2.10}$$

$$a = \frac{25+75}{2} = 50mm,$$

Lead angle γ:

$$\tan(\gamma) = \frac{l}{\pi \times d_w}, \tag{2.11}$$

$$\tan(\gamma) = \frac{16}{\pi \times 25},$$

$$\tan(\gamma) = 0.2037,$$

$$\gamma = 11.51^{\circ},$$

$$\gamma = 0.2008^{C}.$$

Pressure angle: for double start worm pressure angle should not be less than 20° (Bhandari, [19]).

$$\alpha = 20^{\circ}.$$

Addendum of worm h_{aw}:

$$h_{aw} = m = 2.5mm. \tag{2.12}$$

Dedendum of worm h_{fw}:

$$h_{fw} = 1.2 \times m \text{ when } \gamma \leq 15^{\circ}, \tag{2.13}$$

$$h_{fw} = 1.2 \times 2.5 = 3mm,$$

Clearance C:

$$C = h_{fw} - h_{aw}, \tag{2.14}$$

$$C = 3 - 2.5 = 0.5mm.$$

Outside diameter of the worm d_{aw}:

$$d_{aw} = m(q+2), \tag{2.15}$$

$$d_{aw} = 2.5(10+2) = 30.$$

Root diameter of the worm d_{fw}:

$$d_{fw} = d_w - 2h_{fw}\,, \tag{2.16}$$

$$d_{fw} = 25 - 2\times 1.1922 = 22.61\,.$$

Addendum at the throat of worm wheel h_{ag} :

$$h_{ag} = m = 2.5mm\,. \tag{2.17}$$

Dedendum in the median plan h_{fg} :

$$h_{fg} = 1.2\times m\,, \tag{2.18}$$

$$h_{fg} = 1.2\times 2.5 = 3mm\,.$$

Throat diameter of the worm wheel d_{ag} :

$$d_{ag} = d_g + \left(2\times h_{ag}\right)\,, \tag{2.19}$$

$$d_{ag} = 75 + \left(2\times 2.5\right) = 80mm\,.$$

Root diameter of the worm wheel d_{fg} :

$$d_{ag} = d_g - \left(2\times h_{fg}\right), \tag{2.20}$$

$$d_{ag} = 75 - \left(2\times 3\right) = 69mm\,.$$

Face width of worm wheel:

$$F = 2m\times\sqrt{q+1}\,, \tag{2.21}$$

$$F = 2\times 2.5\times\sqrt{10+1} = 16.58mm.$$

Length of the root of the worm wheel teeth l_r :

$$l_r = \left[d_{aw} + 2C\right] sin^{-1}\left[\frac{F}{d_{aw}+2c}\right], \tag{2.22}$$

$$l_r = \left[30 + 2\times 0.5\right] sin^{-1}\left[\frac{16.58}{30+2\times 0.5}\right] = 17.49mm$$

$$l_r \approx 15\ mm\,.$$

Table 1. Dimensions of single stage worm gearbox.

Parameters		Dimensions
i	ratio	*1/15*
Z_w	number of starts of the worm	*2*
Z_g	number of teeth of the worm wheel	*30*
m_n	normal module	*2.5*
m	module	*2.5*
q	diametral quotient	*10 mm*
P_x	axial pitch	*8 mm*
l	lead	*16 mm*
d_w	pitch circle diameter of worm	*25 mm*
d_g	pitch circle diameter of worm wheel	*75 mm*
a	centre distance	*50 mm*
φ	helix angle	*12.52°*
γ	lead angle	*11.51°*
α	pressure angle	*20°*
h_{aw}	addendum of worm	*2.5 mm*
h_{fw}	dedendum of worm	*3 mm*
C	clearance	*0.5 mm*
d_{aw}	outside diameter of the worm	*30 mm*
d_{fw}	root diameter of the worm	*22.61 mm*
h_{ag}	addendum at the throat of worm wheel	*2.5 mm*
h_{fg}	dedendum in the median plan	*3 mm*
d_{ag}	throat diameter of the worm wheel	*80 mm*
d_{fg}	root diameter of the worm wheel	*69 mm*
F	face width of worm wheel	*16.58 mm*
l_r	length of the root of the worm wheel teeth	*15*
	worm wheel bearing	*6008-RS*
N_b	number of ball of bearing	*12*
d	inner diameter of the bearing	*40 mm*
D	outer diameter of the bearing	*68 mm*
B	axial width of the bearing	*15 mm*
θ	the contact angle between the bearing surfaces	*0*
D_B	ball diameter	*9.4 mm*
D_C	cage diameter	*54 mm*

3. The model's development

3.1. Development of three dimensional geometry

The Proe-5 software was used to create the three-dimensional geometry of the worm and the worm wheel as shown in Fig.3. Following are the key dimensions of worms and worm gear: number of starts of the worm $Z_w = 2$, number of teeth of the worm wheel $Z_g = 30$, normal module $m_n = 2.5$, pitch circle diameter of worm $d_w = 25mm$, pitch circle diameter of worm wheel $d_g = 7.5mm$, helix angle $\varphi = 12.52^o$, lead angle 11.51^o, Pressure angle $\alpha = 20^o$, Lead $l = 16mm$.

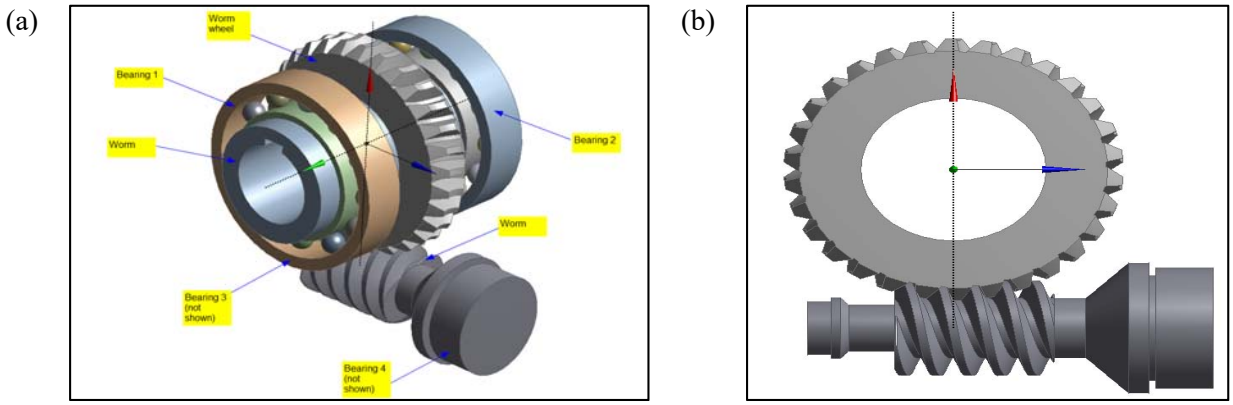

Fig.3. 3-D geometry of worm gear pair: (a) isometric view, (b) side view.

3.2. Development of finite element model

It is very easy to performed analysis of a 3-D model in ANSYS-18 Workbench because of the new ANSYS-18 interface's capability to interface effectively with CAD systems [12]. Model analysis of worm gear pair is carried out by using Ansys workbench 18.0. 3D model is created in Proe-5 is save in STP format file and then imported in the Ansys workbench 18.0. Prior to modal analysis, this work initially sets the material and its specifications. Material details are mention in Tab.2. Number of node *110151* and number of elements *72054* with centre of gravity (*-15*, *0*, *0*) of 3-D model is finalized by Pre-processing tool. Tetra meshing is used for model analysis as shown in Fig.4.

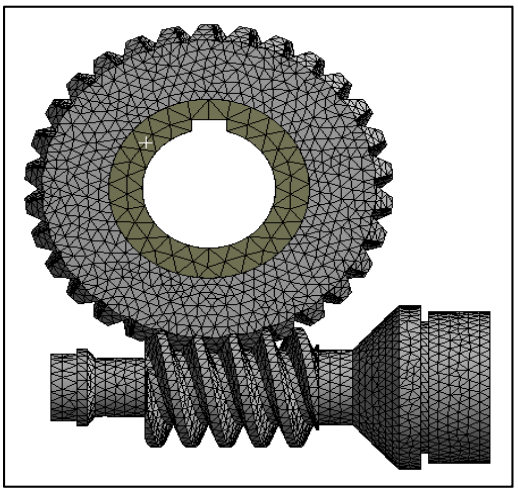

Fig.4. Mesh view of worm gear pair.

Table 2. Material details

Components	**Material**	**Mass**
bearing 1 and 2	steel	not included
worm	steel 304	*0.450*
worm wheel	bronze C104	*0.370*
shaft	steel 304	*0.690*
bearing 3 & 4	steel 304	not included
	Total	*1.51 kg*
material properties	steel	bronze
type/ grade	ASME 304	cast ZcuSn12 (C104 assume)
density	*7850 kg/m^3*	*7580 kg/m^3*
modulus of elasticity	*210 GPa*	*115 GPa*
thermal conductivity	*37.7 W/mK*	*37.7 W/mK*
elongation	*8-10% min*	*8-10% min*
yield strength	*250-310 MPa*	*320-400 MPa*
ultimate strength	*450-600 MPa*	*680-740 MPa*

3.3 Boundary condition of FEA

The outcomes of the analysis will is mainly depends on the use of different constraints, and different constraint conditions will also result in varied modal parameters. Because the worm can only rotate around its own axis (*Z* axis), it is restricted from rotation along the *X*, *Y*, axes and sliding along *X*, *Y* and *Z* axis. The worm wheel can also only rotate around its own axis (*Z* axis), which limits the ability to travel in other directions. In this analysis cylindrical boundary condition (rotational free) was applied on worm and worm wheel bearings as depicted in Fig.5.

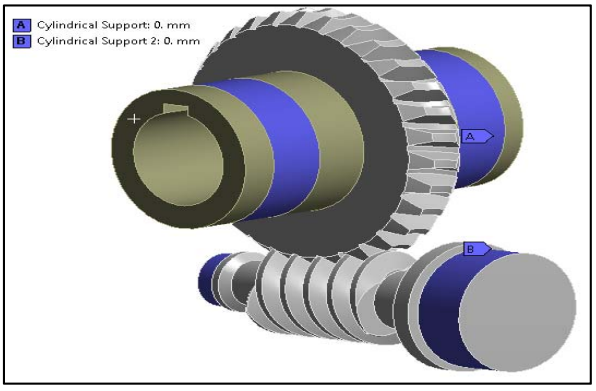

Fig.5. Boundary condition view (cylindrical support, rotational around axial free).

3.4 Experimental test rig

Figure 6 depicts the laboratory experimental test rig implemented in this research work. Experimental test rig consists of a three-phase AC motor with a power output of *0.75 kW* and a rotational speed of *2880 rpm*, ribbon blender worm gearbox having *1/15* reduction speed ratio. The gearbox's speed is adjusted through a variable frequency drive. Rope brake dynamometer loaded the gearbox, and a load cell measured the load. Load applied for experiment is *98.1 N*. Then natural frequencies in conjunction with vibration amplitude are captured for healthy gearbox by using uniaxial accelerometer having sensitivity *100mv/g* mounted in radial direction and 4 channel OR 34 Fast Fourier Transform (FFT) analyser in frequency domain.

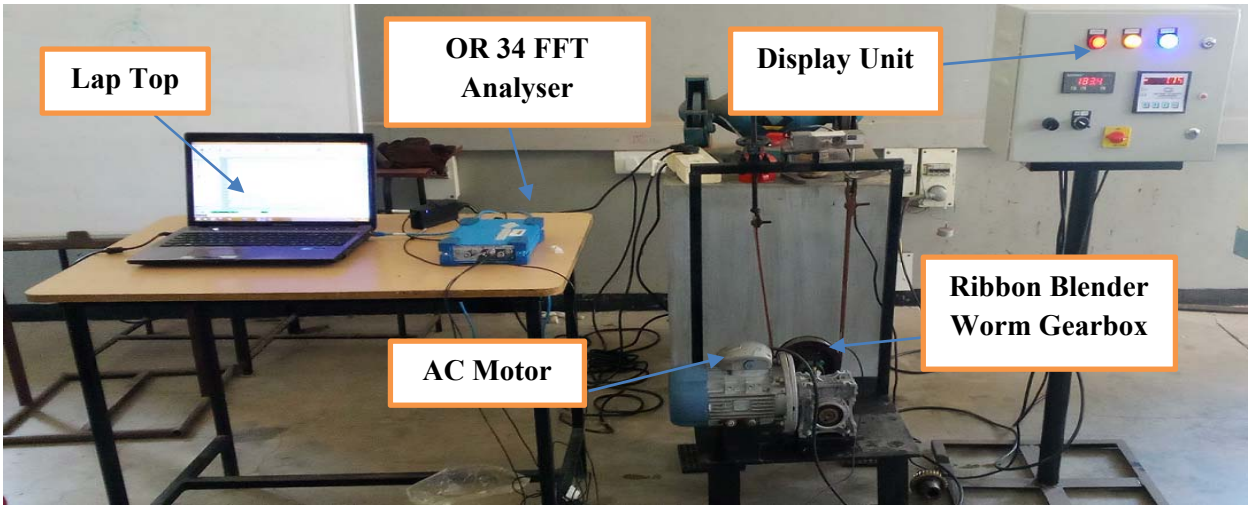

Fig.6 Experimental test-rig.

4. Discussion of Findings

4.1 Modal analysis findings

The vibration features of a structure are estimated numerically using modal analysis, which includes the natural frequency and mode of vibration [10]. In this model analysis, six mode shape of worm gear pair namely (a) worm bending mode, (b) worm wheel bending mode, (c) worm and worm wheel bending mode, (d) worm wheel twisting mode, (e) worm wheel complex bending mode, (f) worm wheel twisting mode were determined which include natural frequency and deformation as shown in Fig.7. Figure 7 (f) shows *143.24 mm* maximum deformation in worm wheel twisting mode vibration and on the other hand Fig.7 (c) shows *63.328 mm* minimum deformation in worm and worm wheel bending mode vibration. Also Fig.7 (f) shows maximum natural frequency i.e *15135 Hz* in worm wheel twisting mode vibration as compared to other mode shape. Therefore results shows that worm wheel vibrates more as compared to worm and worm wheel deteriorate early than worm.

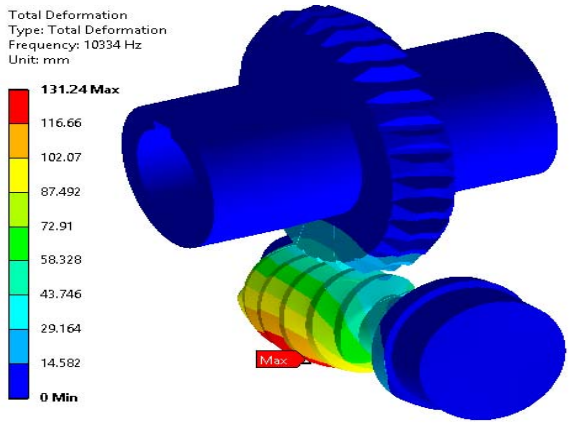

a) Worm bending mode.

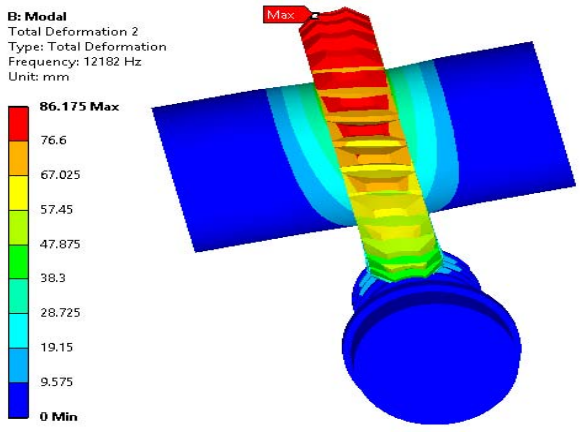

b) Worm wheel bending mode.

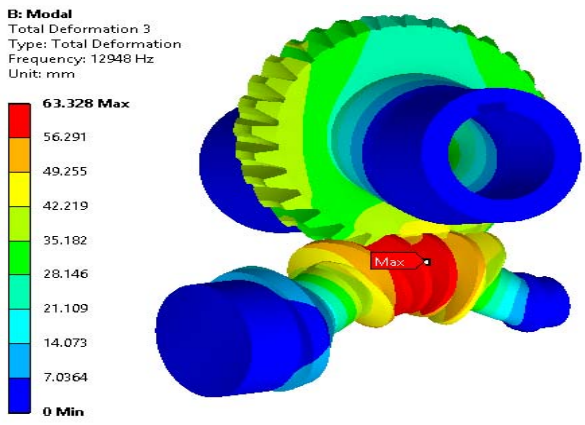

(c) Worm and worm wheel bending mode.

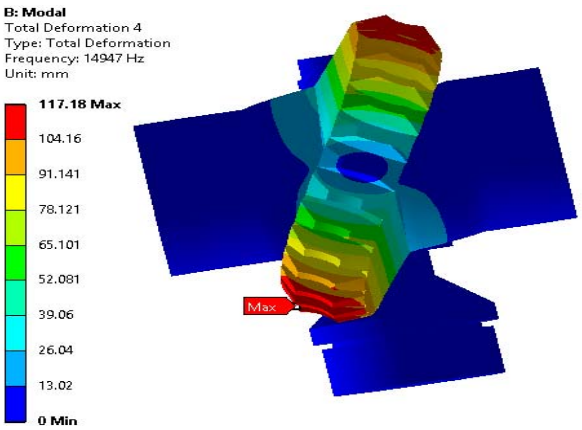

(d) Worm wheel twisting mode.

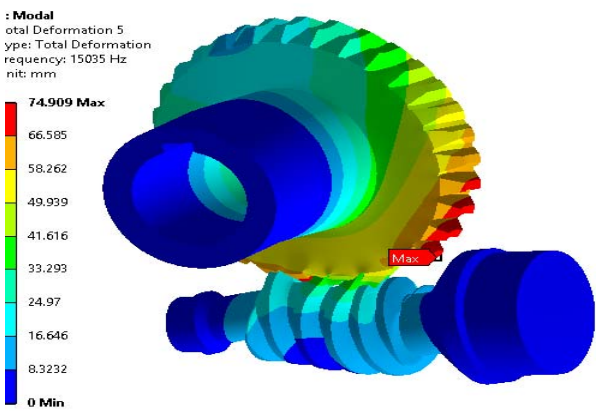

(e) Worm wheel complex bending mode.

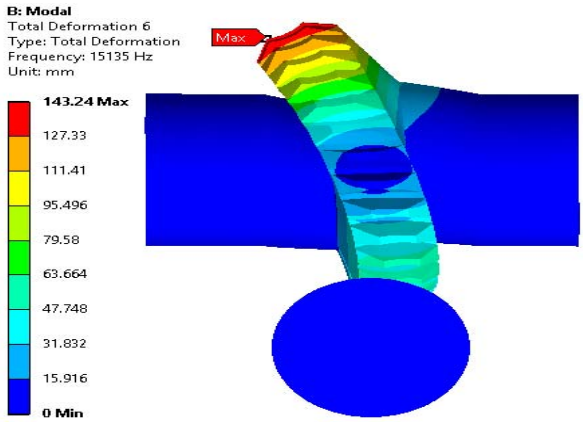

(f) Worm wheel twisting mode.

Fig.7. Model analysis of worm gear pair.

4.2. Experimental findings

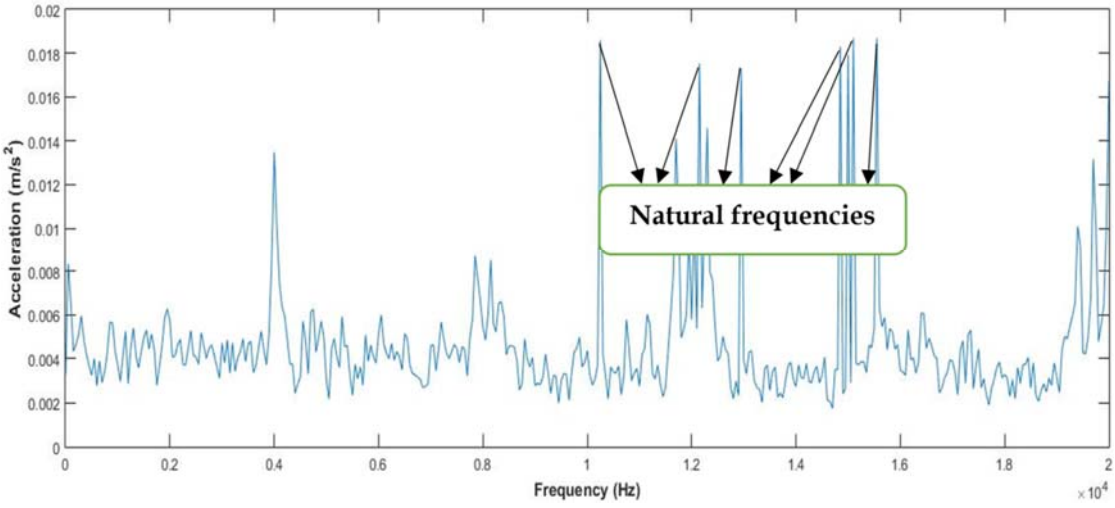

Fig.8. FFT analyser plot.

In order to do the modal analysis, which extracts the natural frequencies together with vibration amplitude, the experiment is performed on a healthy worm gearbox. The worm gearbox FFT analyzer plot is displayed in Fig.8. The FFT analyzer plot shows the six largest amplitudes, which are *0.0186 m/s*^{2}, *0.017913 m/s*^{2}, *0.01753 m/s*^{2}, *0.01731 m/s*^{2}, *0.01829 m/s*^{2}, *0.017913 m/s*^{2}, and *0.01869 m/s*^{2}. Frequency corresponding to highest amplitude is known as natural frequency [7]. Therefore experimental natural frequency are *10250 Hz*, *12150 Hz*, *12950 Hz*, *14850 Hz*, *15000 Hz*, and *15100 Hz*.

4.3. Comparison of modal analysis with experimentation

Based on FEA result and experimental FFT analyser plot, six natural frequencies are nearly equal with error below one percentage as mention in Tab.3. Thus worm gearbox model analysis results are validated through experimentation

Table 3. Comparison of modal analysis with experimentation.

Natural frequency through FEA (Hz)	Natural frequency through experimentation (Hz)	Percentage error (%)
10334	*10250*	*0.81*
12182	*12150*	*0.26*
12948	*12940*	*0.06*
14947	*14850*	*0.65*
15035	*15000*	*0.23*
15135	*15100*	*0.23*

5. Conclusions

In the current model analysis of worm gear pair; finite element analysis is implemented to investigate worm or worm wheel shows early deterioration. Ribbon blender worm gearbox worm gearbox considered for study. Different mode shape like (a) worm bending mode, (b) worm wheel bending mode, (c) worm and worm wheel bending mode, (d) worm wheel twisting mode, (e) worm wheel complex bending mode, (f) worm wheel twisting mode were considered for analysis using Ansys-18 workbench.

Based on the inferences drawn from the study, conclusions are drawn as, in worm gearbox; due to sliding motion take place between worm and worm wheel, the non-stationary vibration produced by worm gear paired. Thus fault detection of worm gearbox by using vibration analysis is challenging task. Model analysis result shows that maximum deformation and natural frequency occurred in case of worm wheel twisting mode vibration. Therefore worm wheel gear get deteriorates early than worm. Research outcome envisages that model analysis plays an important role in further study of vibration analysis of worm wheel. As worm wheel is fails early than worm, worm wheel will consider for fault analysis by using vibration signature.

Acknowledgements

This work is supported by METs Institute of Engineering Management Nashik and Savitribai Phule Pune University, India.

Nomenclature

a – centre distance
C – clearance
d_{ag} – throat diameter of the worm wheel
d_{aw} – outside diameter of the worm

d_{fg} – root diameter of the worm wheel
d_{fw} – root diameter of the worm
d_g – pitch circle diameter of worm wheel
d_w – pitch circle diameter of worm
F – face width of worm wheel
h_{ag} – addendum at the throat of worm wheel
h_{aw} – addendum of worm
h_{fg} – dedendum in the median plan
h_{fw} – dedendum of worm
i – ratio
l – lead
l_r – length of the root of the worm wheel teeth
m – module
m_n – normal module
P_x – axial pitch
q – diametral quotient
Z_g – number of teeth of the worm wheel
Z_w – number of starts of the worm
α – pressure angle
γ – lead angle
φ – helix angle

Worm wheel bearing

B – axial width of the bearing
d – inner diameter of the bearing
D – outer diameter of the bearing
D_B – ball diameter
D_C – cage diameter
N_b – number of ball of bearing
θ – the contact angle between the bearing surfaces

References

[1] Hassan A.R., Thanigaiyarasu G. and Ramamurti V. (2008): *Effects of natural frequency and rotational speed on dynamic stress in spur gear*.– World Academy of Science, Engineering and Technology, vol.6, No.12, pp.12-20, https://www.researchgate.net/publication/328759949
[2] Kurbet R., Doddaswamy V., Amruth C.M., Kerur M.H. and Ghanaraja S. (2022): *Frequency response analysis of spur gear pair using FEA*.– Materials Today Proceedings, vol.52, No.4, pp.2327-2338, https://doi.org/10.1016/j.matpr.2021.12.517
[3] Mailapalli R. and Sharief S.H. (2017): *Design and assembly analysis of a worm-assembly in a gear box*.– IJMETMR, vol.4, No.4, pp.85-95.
[4] Mailapalli H.G. and Maniya K.D. (2020): *Experimental investigation of churning power loss of single start worm gear drive through optimization technique*.– Materials Today Proceedings, vol.28, No.4, pp.2031-2038, https://doi.org/10.1016/j.matpr.2019.12.365
[5] Hizarci B., Umutlu R.C., Kiral Z. and Ozturk H. (2021): *Fault severity detection of a worm gearbox based on several feature extraction methods through a developed condition monitoring system*.– SN Applied Sciences, vol.3, No.129, pp.129-140, https://doi.org/10.1007/s42452-020-04131-w
[6] Waqar T. and Demetgul M. (2016): *Thermal analysis MLP neural network based fault diagnosis on worm gears*.– Measurement, vol.86, No.5, pp.56-66, https://doi.org/10.1016/j.measurement.2016.02.024.

[7] Karabacak Y.E., Ozmen N.G. and Ozmen L. (2020): *Worm gear condition monitoring and fault detection from thermal images via deep learning method*.– Maintenance and Reliability, vol.22, No.3, pp.544-556. https://doi.org/10.17531/ein.2020.3.18.
[8] Umutlu R.C., Hizarci B., Kiral Z. and Ozturk H. (2020): *Classification of pitting fault levels in a worm gearbox using vibration visualization and ANN*.– Sadhana Academy Proceedings in Engineering Sciences, vol.45, No.22, pp.1-13. https://doi.org/10.1007/s12046-019-1263.
[9] Londhe R.R., Shitole J. S. and Valkunde B.R. (2021): *Bending stress analysis of worm wheel of winch machine gearbox using experimental and FE analysis*. IJARIIE, vol.7, No.4, pp.2210-2229, https://doi.org/10.1016/j.matpr.2022.09.089.
[10] Honkalas R., Deshmukh B. and Pawar P. (2023): *Investigation and analysis of existing design of worm and worm wheel of a gear motor used in a soot blower*.– Materials Today Proceedings, vol.72, No.3, pp.904-910.
[11] Jibhakate R.A., Thakare P.S., Choudhari C.J. and Patil P. (2022): *Estimation of natural frequencies of gear meshing system using modal analysis*.– Springer Proceedings in Energy, vol.1, pp.893-902. https://link.springer.com/chapter/10.1007/978-981-16-6875-3_71
[12] Bhat J.S., Sonawane B.U. and Desai M.R. (2020): *Finite element analysis of tribological properties of worm gear under wet condition*.– IJAST, vol.29, No.8s, pp.5238-5243, http://sersc.org/journals/index.php/IJAST/article/view.
[13] Mohamed A.S., Sassi S. and Paurobally M.R. (2018): *Model-based analysis of spur gears dynamic behavior in the presence of multiple cracks*.– Shock and Vibration, vol.2018, No.1, pp.1-21, https://doi.org/10.1155/2018/1913289
[14] Maheedhara S.S. and Pourboghrat F. (2007): *Finite element analysis of composite worm gears*.– JTCM, vol.20, No.1, 27-51, DOI: 10.1177/0892705707068818
[15] Patil P.J., Patil M.S. and Joshi K.D. (2017): *Dynamic state or whole field analysis of helical gear*.– J. Inst. Eng. India Ser. C, vol.100, pp.37-42, DOI 10.1007/s40032-017-0389-3
[16] Dr. Ganesh E.N. (2022): *Simulation of the 3d model of worm gear using finite element analysis*.– Global Journal of Research in Engineering & Computer Sciences, vol.2, pp.1-6. DOI: 10.5281/zenodo.6386441
[17] Tao Z., Chen H., Zhang X. and Jiang Y. (2021): *Failure analysis of worm gear in worm transmission*.– Journal of Physics: Conference Series, vol.1965, pp.1-9, doi:10.1088/1742-6596/1965/1/012132
[18] Bhandari V.B. (2009): *Design of Machine Element*, 2nd ed.– Tata McGraw-Hill, New Delhi, India.

Received: February 2, 2024
Revised: April 2, 2024